




# Intravital Monitoring of Vasculature After Targeted Gene Therapy Alone or Combined With Tumor Irradiation

Technology in Cancer Research & Treatment  
Volume 17: 1-8  
© The Author(s) 2018  
Reprints and permission:  
sagepub.com/journalsPermissions.nav  
DOI: 10.1177/1533033818784208  
journals.sagepub.com/home/tct  


Monika Savarin, PhD<sup>1</sup> , Ajda Prevc, MSc<sup>1</sup>, Matic Rzek, BEng<sup>2</sup>, Masa Bosnjak, PhD<sup>1</sup>, Ilija Vojvodic, MSc<sup>3</sup>, Maja Cemazar, PhD<sup>1,4</sup> , Tomaz Jarm, PhD<sup>2</sup>, and Gregor Sersa, PhD<sup>1,5</sup> 

## Abstract

Vascular-targeted therapies exhibit radiosensitizing effects by remodeling tumor vasculature, thus facilitating the increased oxygenation of the remaining tumor tissue. To examine these phenomena, the effects of antiendoglin gene therapy alone and in combination with irradiation were monitored for 5 consecutive days on a murine mammary adenocarcinoma (TS/A) tumor model growing in a dorsal window chamber. The vascularization of the tumors was assessed by the determination of the tumor vascular area and by measurement of tumor perfusion by using laser Doppler flowmetry to provide insight into intratumoral gene electrotransfer effects. The changes in the vascular area after this specific therapy correlated with laser Doppler measurements, indicating that either of the methods can be used to demonstrate the induced changes in the vascularization and perfusion of tumors. Gene electrotransfer with an endothelial-specific promoter resulted in a vascular-targeted effect on tumor vasculature within the first 24 hours and did not restore within 5 days. The combination with the irradiation did not result in a more pronounced vascular effect, and irradiation alone only abrogated the formation of new vessels and prevented an increase in the tumor perfusion over time. The results indicate that tumors grown in a dorsal window chamber facilitate intravital measurements of the vascularization of tumors and blood perfusion, enabling the monitoring of the antiangiogenic or vascular disruptive effects of different therapies.

## Keywords

vascular targeted therapy, gene therapy, intravital microscopy, microcirculation measurement, endoglin, irradiation

## Abbreviations

EP, electroporation; GET, gene electrotransfer; GFP, green fluorescent protein; IR, irradiation; IR + EP, electroporation and irradiation; IR + GET, gene electrotransfer and irradiation; IR + TS, injection of therapeutic plasmid and irradiation; LDF, laser Doppler flowmetry method; RGB, bright-field images; TS, therapeutic plasmid; VEGF, vascular endothelial growth factor.

Received: December 22, 2017; Revised: March 27, 2018; Accepted: May 24, 2018.

## Introduction

Vascular-targeted therapies in cancer treatment show great promise. Combining these therapies with radiotherapy can have good radiosensitizing effects that are important for the treatment of radioresistant tumors. With antiangiogenic agents, the development and growth of abnormal tumor vasculature can be prevented, and the tumors therefore remain smaller and well oxygenated. However, with vascular-disrupting agents, the abnormal tumor vasculature of bigger and heterogenic tumors is damaged, causing a necrotic tumor center and viable, well-oxygenated tumor rim. The increased oxygenation of

<sup>1</sup> Department of Experimental Oncology, Institute of Oncology Ljubljana, Ljubljana, Slovenia

<sup>2</sup> Department of Biomedical Engineering, Faculty of Electrical Engineering, University of Ljubljana, Ljubljana, Slovenia

<sup>3</sup> Division of Radiotherapy, Institute of Oncology Ljubljana, Ljubljana, Slovenia

<sup>4</sup> Faculty of Health Sciences, University of Primorska, Izola, Slovenia

<sup>5</sup> Faculty of Health Sciences, University of Ljubljana, Ljubljana, Slovenia

## Corresponding Author:

Gregor Sersa, PhD, Department of Experimental Oncology, Institute of Oncology Ljubljana, Zaloska 2, SI-1000 Ljubljana, Slovenia.

Email: gsertsa@onko-i.si



tumors is the key element of radiosensitization; therefore, the combination of these 2 treatment approaches is of great importance for achieving better tumor responses.<sup>1-5</sup>

Several preclinical and clinical studies on targeting tumor vasculature, predominantly by blocking vascular endothelial growth factor (VEGF) and its receptors, have been reported. The therapeutic outcomes are promising, although the development of anti-VEGF drug resistance and side effects are frequent due to the poor specificity of the target and the antibodies used.<sup>1,2</sup> Therefore, the search for other molecular targets in angiogenesis signaling pathways continues. One of the promising new targets is endoglin, a transforming growth factor  $\beta$  coreceptor involved in a complex signaling pathway of endothelial cells. In previous studies, we showed that silencing endoglin expression by the electrotransfer of therapeutic plasmid (TS), that is, gene electrotransfer (GET), leads to significant antitumor effectiveness due to both antiangiogenic and vascular-disrupting effects.<sup>6</sup> Combined with tumor irradiation (IR), good radiosensitization was observed. However, the percentage of total tumor-free mice depends on the tumor model used.<sup>4,5</sup> Vascular-targeted effectiveness was confirmed by histological analyses of tumors at a specific time point (day 6); nevertheless, the precise time scale of events remains unclear.

For the *in vivo* real-time observation of vascular-targeted effects, intravital microscopy is the most appropriate observational tool at a single vessel level. This technique enables the acquisition of multiple parameters at the same time point and facilitates daily noninvasive monitoring of changes in the same animal.<sup>7</sup> To further obtain and evaluate the specific vascular effects on the blood flow in microcirculation, laser Doppler flowmetry can be used noninvasively.<sup>8-10</sup> To elucidate the effects of intratumoral vascular-targeted gene therapy of silencing endoglin expression, we used these 2 noninvasive methods on a dorsal window chamber model and compared the obtained results and calculated their correlation. To distinguish the effects of the GET on tumors and vasculature, we selected a murine mammary adenocarcinoma (TS/A) tumor model, in which endoglin is expressed only in endothelial cells but not in tumor cells. To monitor radiosensitization, the tumors were also irradiated and compared with other groups.

## Materials and Methods

### Cell Line, Plasmids, and Drugs

A green fluorescent protein (GFP)-expressing murine mammary adenocarcinoma TS/A cell line (TS/A GFP) was used in the experiments for induction of the subcutaneous tumors.<sup>11</sup> The TS/A cell line<sup>12</sup> was tested for authentication in 2017 at the IDEXX BioResearch (Ludwigsburg, Germany). The cells were cultured in advanced minimum essential medium (Gibco, Thermo Fisher Scientific, Waltham, Massachusetts) supplemented with 5% fetal bovine serum (Gibco), 10 mM L-glutamine (GlutaMAX; Gibco), 2 mg/mL Geneticin (Gibco), 50  $\mu$ g/mL gentamicin (Krka, Novo Mesto, Slovenia), and 100

U/mL penicillin (Grünenthal, Aachen, Germany) in a 5% CO<sub>2</sub> humidified incubator at 37°C.

A plasmid encoding short hairpin RNA (shRNA) for endoglin silencing with a tissue-specific polymerase II promoter for endothelial cell marker endothelin-1 (pET-antiCD105; TS) was used as a TS.<sup>5</sup> The amplification of both plasmids was performed in competent *Escherichia coli* (JM107; Invitrogen, Thermo Fisher Scientific, Waltham, Massachusetts).

The plasmids were isolated using the JETSTAR 2.0 Endotoxin-Free Plasmid MEGA Kit (Genomed, Löhne, Germany) and diluted in endotoxin-free water to a concentration of 4  $\mu$ g/ $\mu$ L. The plasmid concentration was measured with a spectrophotometer at 260 nm (Take3 Micro-Volume Plate, Epoch Microplate Spectrophotometer; BioTek, Bad Friedrichshall, Germany) and purity was determined by agarose gel electrophoresis and measurements of the absorbance ratio at 260 and 280 nm.

### Experimental Animals

For the experiments, 8- to 14-week-old female BALB/c mice (Envigo, Udine, Italy) were used and maintained under specific pathogen-free conditions at a constant room temperature, humidity, and 12-hour light and 12-hour dark cycle, and food and water were provided *ad libitum*. Prior to the experiments, the animals were subjected to an adaptation period of 2 weeks. The animal studies were performed in accordance with the guidelines for animal experiments of the European Union (EU) directive, and approval was obtained from the Ministry of Agriculture and the Environment of the Republic of Slovenia (Permission No. 34401-3/2012/2) based on the approval of the National Ethics Committee for Experiments on Laboratory Animals.

### Implantation of the Dorsal Window Chamber

Before the dorsal window chamber implantation, the mice were anesthetized with an intraperitoneal injection of anesthetic solution (ketamine, 1 mg/mL, Narketan; Vetoquinol, Ittigen, Switzerland; xylazine 5 mg/mL, Chanazine; Chanelle Pharmaceuticals, Loughrea, Ireland; acepromazine 0.4 mg/mL, PromAce; Fort Dodge Animal Health, Fort Dodge, Iowa) adjusted to the weight of the animals (in a range of 70-90  $\mu$ L: 3.7  $\mu$ L/g). Subsequently, the skin on the back of the mouse was shaved and depilated with depilatory cream (Vitaskin; Krka), and the dorsal window chamber (APJ Trading, Ventura, California) was surgically implanted. The entire surgical procedure was performed under aseptic conditions, and the animals were warmed up with heating pads. First, the 2 titanium frames were attached onto the extended double layer of the skin with stainless-steel screws and silk sutures. Subsequently, one layer of the skin was excised, while all fat and connective tissues in the other layer of the skin were dissected away to ensure optimal microscopic observation of the vasculature. The dorsal window chamber was filled with physiological solution and closed with a 12-mm cover glass (Glaswarenfabrik Karl

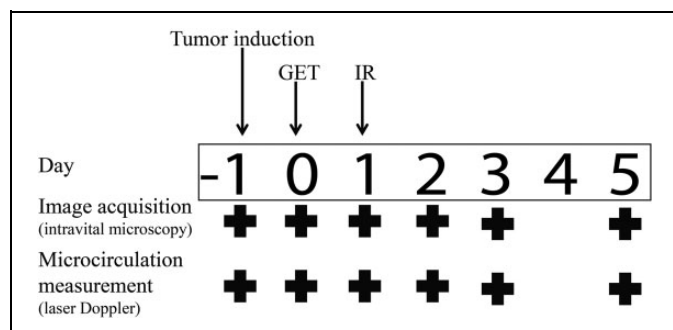


**Figure 1.** A schedule of experimental design and data acquisition. GET indicates gene electrotransfer; IR, irradiation, +, method used at a specific day.

Hecht, Sondheim, Germany). To provide analgesia after surgery and on the following day, the mice were intramuscularly injected with 50  $\mu$ L of butorphanol (0.3 mg/kg, Torbugesic; Fort Dodge Animal Health).

### Tumor Induction and Therapy

Two days after surgery, a suspension of  $7 \times 10^5$  TS/A GFP tumor cells in 5  $\mu$ L of physiological solution was injected into the lower layer of the skin. The next day (day 0), the experiment was performed on viable tumors in the dorsal window chamber, as assessed with intravital microscopy prior to the experiment. During tumor induction, therapeutic procedures, and monitoring of therapeutic effectiveness, the animals were anesthetized with inhalation anesthesia (isoflurane; Nicholas Piramal India Ltd, Mumbai, India) and placed on custom-designed holders.

*Gene electrotransfer* (Figure 1) was performed on day 0. After intratumoral injection of 5  $\mu$ L (4  $\mu$ g/ $\mu$ L) of the plasmid (20  $\mu$ g in total), the electric pulses were delivered through 2 parallel stainless-steel electrodes with a 4-mm interelectrode distance. The electric pulses were generated by electroporator ELECTRO cell B10 (LEROY biotech, L'Union, France). Eight square-wave pulses were applied in 2 sets of 4 pulses in perpendicular directions at a frequency of 1 Hz, an amplitude over distance ratio of 600 V/cm, and a duration time of 5 milliseconds.

The tumors were locally irradiated 1 day after GET (day 1), with a single dose of 5 Gy, at a dose rate of 1.41 Gy/min, using a Gulmay D3300 GM0159 IR unit (Gulmay Medical Ltd, Shepperton, United Kingdom) operating at 200 kV, 10 mA, with 1.0-mm copper filtration, 20-mm circular applicator, and 300-mm distance from the focus to the skin. During IR, the animals and nontumor fields of the dorsal window chamber were shielded and restrained in special lead holders with apertures, facilitating only the IR of the tumor area and protecting the rest of the animal.

### Experimental Groups

To observe and determine the therapeutic effectiveness of the treatments, the animals were divided into 12 groups as follows:

- To determine the nonspecific effects, the tumors in control groups were injected with only H<sub>2</sub>O or a TS (pET-antiCD105).
- With electrotransfer as a delivery method, the injections were combined with electric pulses as described above, forming groups of electroporation (EP; injection of H<sub>2</sub>O followed by electric pulses) and GET of TS (GET; injection of TS followed by electric pulses).
- To elucidate the IR contribution, all of the groups described above were combined with the same IR dose, forming the groups of irradiation alone (IR) or combined with the injection of TS (IR + TS), application of EP (IR + EP) or GET (IR + GET).

All groups comprised 3 animals per group, and the principle of 3 R of animal welfare (reduction of animal number, refinement of the experiments, and replacement of animals with other models) was obtained.

### Image Acquisition and Analysis

The dorsal window chambers were monitored daily with intravital microscopy using a Carl Zeiss SteREO Lumar V12 (Carl Zeiss, Jena, Germany) fluorescence stereomicroscope equipped with a NeoLumar S 0.8 $\times$  objective (Carl Zeiss) and a AxioCam MRc5 digital camera (Carl Zeiss). From the anesthetized animals at room temperature, bright-field images (RGB) of window chambers were taken every 24 hours to observe changes in the formation and morphology of the blood vessels. On day 5, which was 6 days after the tumor induction, red fluorescence of blood vessels was visualized after the intraorbital injection of rhodamine B-labeled dextran (70 kDa; Sigma-Aldrich, St. Louis, Missouri; filters used for excitation 525-575 nm and emission 570-640 nm), in contrast with green fluorescence from tumors (GFP; filters used for excitation 450-490 nm and emission 500-550 nm). To measure the area of the blood vessels, binary masks were generated from bright-field images acquired at 50 $\times$  magnification. The original image was processed with a low-pass filter and the threshold RGB value was determined to discriminate between the blood vessels and the surrounding tissue (the pixels belonging to the blood vessels were given a value of 1, all other pixels below the threshold were given a value of 0). Binary masks of the obtained blood vessels were thereafter superimposed over the original image, and discrepancies between the blood vessels network on the original image and the binary mask were manually corrected. From the corrected binary masks, the area of blood vessels was estimated with image analysis software (AxioVision, Carl Zeiss).

### Microcirculatory Blood Flow Measurements

During the measurements of tumor microcirculation, following the image acquisitions of dorsal window chamber, the animals were anesthetized by isoflurane inhalation, placed on an automatically regulating heating pad, connected with a rectal

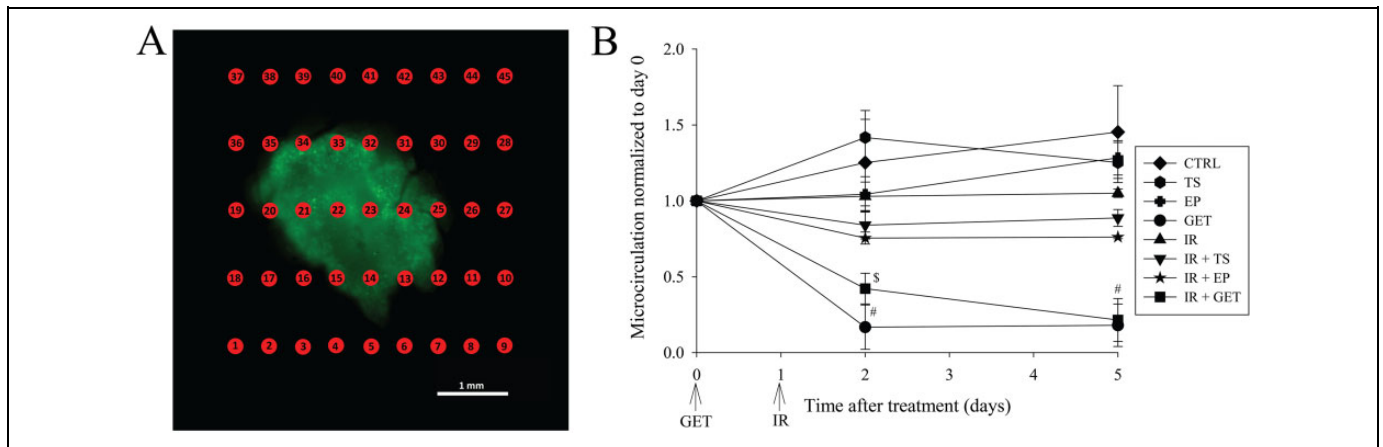


**Figure 2.** Microcirculation measurements on a dorsal window chamber model. A, Display of measuring points and their distribution. Scale bar = 1 mm. B, The tumor microcirculation analyzed from the measuring points from the tumor area. The results represent the AM  $\pm$  SEM,  $n = 10$ -40 measuring points in a viable part of the tumors.  $\$P < .05$  versus CTRL, TS, EP, IR;  $\#P < .05$  versus all the groups instead of GET (TS) and IR + GET (TS) themselves. AM indicates arithmetic means; CTRL, control; EP, electroporation; GET, gene electrotransfer; IR, irradiation; SEM, standard errors; TS, therapeutic plasmid.

temperature probe to prevent hypothermia, and fixed on a custom-made holder to prevent the dorsal windows from moving. The measurements were performed daily at the same time of day and in the same measurement locations. Microcirculation was measured using the laser Doppler flowmetry method (LDF). In LDF, the quantification of Doppler shift effect (ie, changes in the wavelength of a laser light photons scattered on moving erythrocytes in vasculature) is used to monitor the changes in relative blood flow in the microcirculatory network comprising capillaries, arterioles, and venules.<sup>13</sup>

The PeriFlux System 5000 (Perimed, Järfälla, Sweden) was used with probe type 407 with the external radius of 1 mm and 2 optical fibers separated by 250  $\mu\text{m}$ . To reach a depth of 0.5 to 1 mm into the skin for noninvasive measurements of microcirculation, a laser light with a 780 nm wavelength was implemented in this instrument. The signals of microcirculation were measured in 45 points distributed in a rectangular grid (9 by 5 points) covering the entire tumor area plus its immediate tumor-free surrounding. On the x-axis, the distance between the points was 0.5 mm, whereas on the y-axis, the distance between the points was 1 mm (Figure 2A). The LDF probe was fixed inside the 3-axis micromanipulator, which enables controlled movements of the probe tip, without physically touching the tissue. Correct initial positioning of the probe tip with respect to the grid of measurement points was assured by using the reference points indicated on the window frame chamber on day 0, enabling repeatable movements through all measurement points. For each measurement point, the relative microcirculatory blood flow (expressed in relative perfusion units) was determined as the average of the signal level within the most stable 30 seconds long segment selected from the 50-second-long interval. In the analysis, only the measurement points located over the tumor area were considered. The average of all measuring points above the tumor was used for the

estimation of relative perfusion in the entire tumor on the given day. The number of measurement points used for a particular tumor was adjusted daily according to the progression or inhibition of the tumor growth, thus ranging between 10 and 40 points. All signal processing was performed using Matlab software (Mathworks, Natick, Massachusetts).

### Statistical Analysis

Data were tested for normality of distribution with the Shapiro-Wilk test and represented as arithmetic means, with error bars representing standard errors. The difference between the groups was evaluated by 1-way analysis of variance, followed by a Holm-Sidak test for multiple comparisons. A  $P$  value of less than .05 was considered statistically significant. The linear correlation between the results of the 2 methods was evaluated by the Pearson correlation coefficient. SigmaPlot software (Systat Software, Chicago, Illinois) was used for statistical analysis and graphical representation.

## Results

### Intravital Microscopy Confirms the Vascular-Targeted Effectiveness of Gene Therapy Silencing Endoglin

*In vivo*, by using intravital microscopy on a dorsal window chamber model, we directly and noninvasively monitored the effectiveness of the GET for 5 consecutive days after the therapy. The study was performed on a TS/A tumor model, stably transfected with GFP, which does not express endoglin,<sup>11</sup> to elucidate the effectiveness of this gene therapy on the vasculature.

In the control group, where tumors were not treated, the tumor vasculature was growing and forming a complex network over time, which resulted in a  $175.1\% \pm 14.3\%$  increase of the tumor blood vessel area from pretreatment to the last day

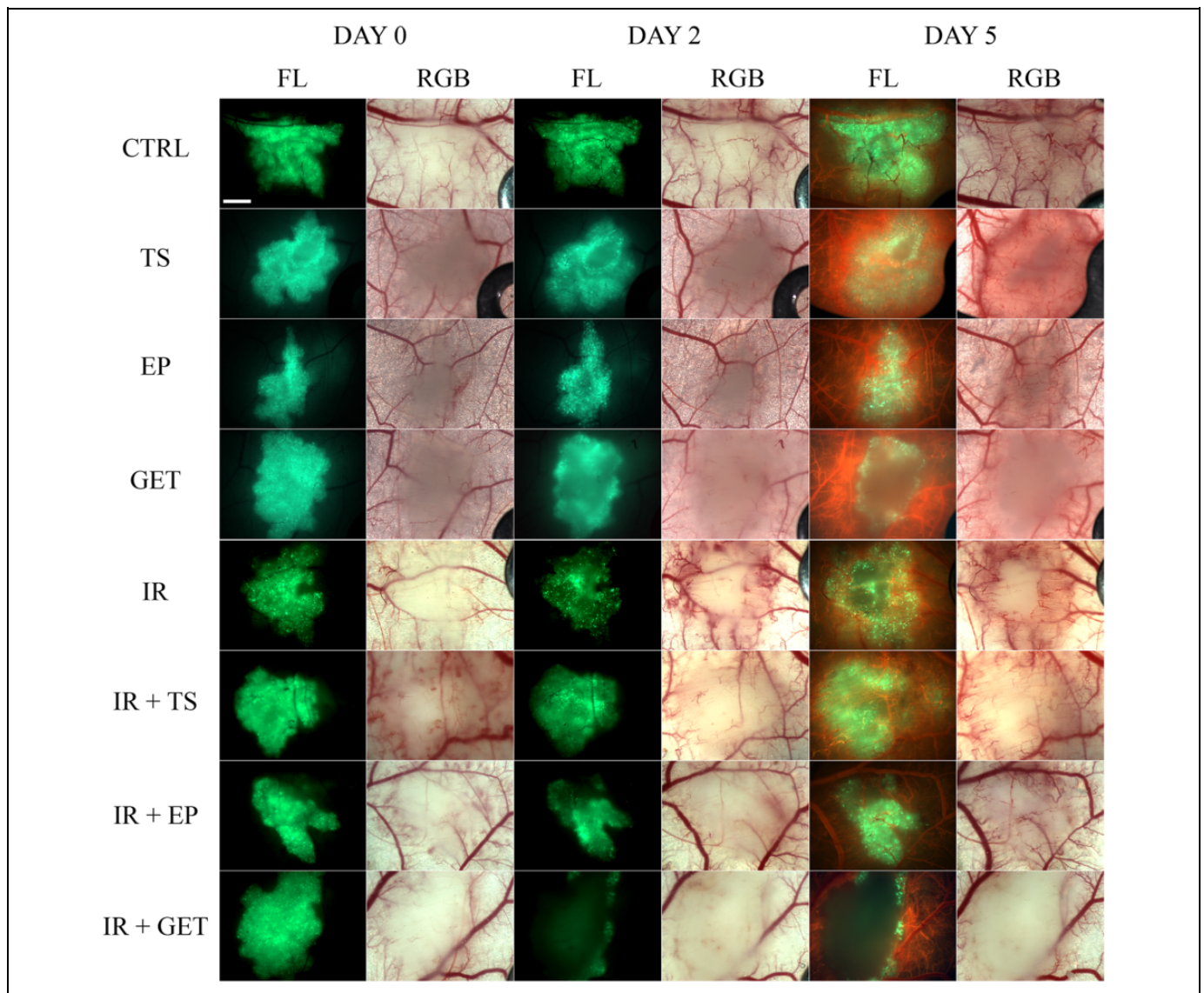


**Figure 3.** Gene electrotransfer of plasmid silencing endoglin expression promotes vascular-targeted effects. Bright-field (RGB) images of tumors and their vasculature in a dorsal window chamber model before (day 0) and after (day 2 and 5) the therapy and FL images of tumors (green) and vasculature (red, day 5). Scale bar = 1 mm. CTRL indicates control; FL, fluorescence; EP, electroporation; GET, gene electrotransfer; IR, irradiation; IR + TS, injection of TS and irradiation; IR + EP, electroporation and irradiation; IR + GET, gene electrotransfer and irradiation; TS, therapeutic plasmid.

of observation, thereby enabling tumors to grow and maintain their viability. In the groups where tumors were irradiated (IR, IR + TS, IR + EP), the blood vessel area within the 5-day observation period was not significantly reduced, and only minor vascular changes were observed. In contrast, the GET induced a statistically significant reduction in the tumor vessel area. This effect was already observed at 24 hours after the therapy, when the blood vessel area was reduced to  $41.0\% \pm 4.8\%$  of the pretreatment value. The same scale of vascular reduction was present also when the GET was combined with irradiation (IR + GET), indicating that IR did not further promote vascular destruction. In both groups, vascular-targeted effects were observed: GET destroyed the existing vessels in

the treated area (Figure 3) and prevented the formation of new tumor vasculature (Figure 4).

In addition to the changes in the tumor vasculature, tumor viability was also affected in the groups with GET alone (GET) or in a combination with irradiation (IR + GET). The lack of tumor viability, resulting in non- or poorly fluorescent tumors, steadily diminished from the beginning of the therapy until the last day of the observation. These results indicate tumor cell death due to deprivation of blood flow, oxygen, and nutrients, which was observed also in our previous study, where the tumor volume was measured.<sup>4</sup> Furthermore, the therapy had no effect on the surrounding tissue and vasculature, suggesting a specificity of the plasmid promoter for the activated endothelial cells.



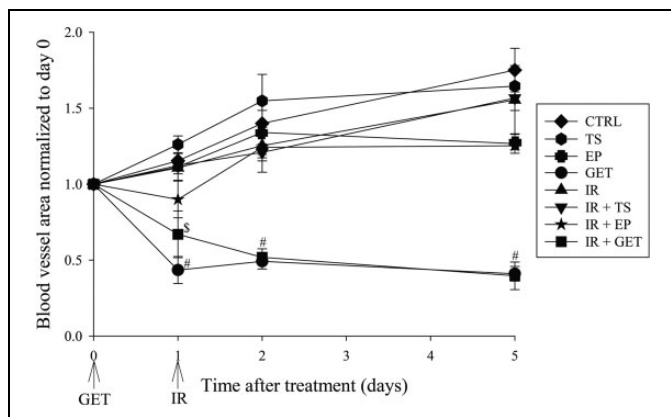


**Figure 4.** The area of tumor vasculature was reduced after therapeutic gene electrotransfer. Blood vessel area analyzed from the bright-field images of the dorsal window chamber model. All values were normalized to the value of day 0. The results represent the AM  $\pm$  SEM, consisting of  $n = 3$  animals per experimental group.  $\$P < .05$  versus CTRL, TS, EP, IR, IR + TS;  $\#P < .05$  versus all the groups except GET and IR + GET themselves. AM indicates arithmetic means; CTRL, control; EP, electroporation; GET, gene electrotransfer; IR, irradiation; SEM, standard errors; TS, therapeutic plasmid.

### Reduction in Microcirculation Is Promoted in Therapeutic Groups

The microcirculation in the tumors was measured as a relative change in microcirculatory blood flow by using laser Doppler flowmetry. This technique was the second noninvasive method used daily on the dorsal window chamber model to evaluate the effectiveness of the therapeutic gene therapy targeting tumor vasculature.

The results of the measurements of the blood flow can be divided into the following 3 categories for the response (Figure 2B). In the nontreated groups, an increase in blood microcirculation was observed, likely due to the activation of different growth factors in the tumor microenvironment and the consequent formation of the tumor vasculature. The second group comprised variants with IR (IR, IR + TS, IR + EP), where blood flow remained at the same level as that at the beginning of the therapy. These results indicate that IR delays angiogenesis. In the third group, where GET was used with or without IR, both vascular-targeted effects (antiangiogenic and vascular targeted) were indicated. Here, microcirculation was significantly reduced on the first day after GET and did not recover (or even further decrease) up to the last day of observation.

### Correlation Between 2 Noninvasive Methods

In the dorsal window chamber, 2 methods were used and compared: a morphological measurement of the area of tumor vasculature and a physiological measurement of the tumor blood flow. Using these 2 methods, we independently confirmed that GET prevents the formation of new tumor vasculature and destroys the existing vasculature. This effect was already observed the day after therapy, regardless of whether

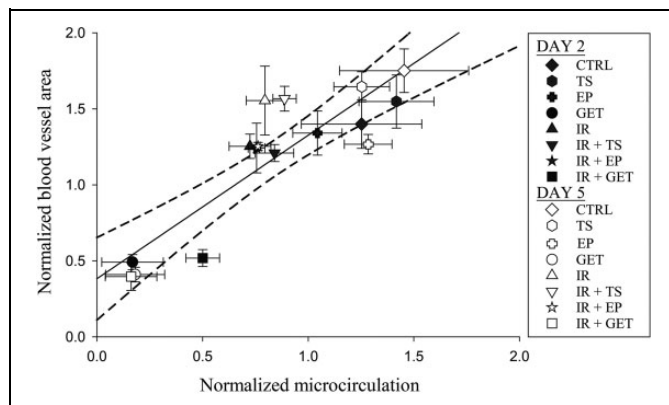


**Figure 5.** Correlation of the results obtained from blood vessel area and microcirculation measurement. All values were normalized to day 0. The results represent the AM  $\pm$  SEM, consisting of the measurements average of blood vessel area and/or microcirculation, normalized to day 0, as previously described. The bands represent the results of linear regression with the 95% of confidence interval (Pearson correlation [ $R = 0.882$ ];  $y = a \times x + y_0$  [ $a = 0.944$ ;  $P < .0001$ ;  $y_0 = 0.383$ ;  $P = .0091$ ]). AM indicates arithmetic means; SEM, standard errors.

electrotransfer was performed alone or in combination with IR. Furthermore, IR resulted in a minor modulating effect on the vasculature, while in the control group, vasculature was formed over time. The high correlation of the 2 methods on day 2 (correlation coefficient [ $R = 0.900$ ;  $P = .002$ ;  $n = 8$ ], day 5 ( $R = 0.881$ ;  $P = .004$ ;  $n = 8$ ), or all the data together ( $R = 0.882$ ;  $n = 16$ ) indicates that these methods complement each other, and either technique could be used to monitor the vascular effects and predict the changes occurring at other levels (Figure 5).

### Discussion

Silencing endoglin expression with GET alone or in combination with IR caused significant tumor regression, promoted by vascular-targeted effects, that is, both antiangiogenic and vascular-disrupting effects. The therapeutic effectiveness was observed at 24 hours after GET and persisted until the last day of the observation. This phenomenon was observed in a dorsal window chamber model by using 2 noninvasive methods: intravital microscopy to monitor the blood vessel area and laser Doppler flowmetry to measure the microcirculation of tumors. A good correlation between the results of both methods was observed, indicating that by measuring the blood vessel area, we can predict the net microcirculatory blood flow in tumors and vice versa. The results obtained with 2 independent noninvasive methods additionally confirmed the previous histological observations evaluating hypoxia, apoptosis, proliferation, vascularization, and necrosis,<sup>4,5</sup> providing detailed insight into the tumor microenvironment.

The dorsal window chamber model facilitates the daily intravital and noninvasive monitoring of multiple parameters of tumors and their vasculature. Tumor vasculature is a key factor for promoting tumor growth and development, since it

can activate different factors that modulate tumor microenvironment.<sup>14</sup> For tumors in nontreated groups, growing in a dorsal window chamber model, the tumor size and viability increased daily due to the growth and development of the tumor vasculature; this increase was also reflected in the increased blood flow through the tumor. In the groups that included IR (IR, IR + TS, IR + EP), the blood vessel area persisted at the same level as that detected at the beginning of the observation. This effect was additionally confirmed by microcirculation measurements, indicating the transient effectiveness of IR on the tumor vasculature, rather than the tumor cells directly, since the viability of tumors remained unchanged. In a previous study, we showed that targeting radioresistant TS/A tumors<sup>15</sup> with vascular-targeted GET can promote the radiosensibilization of tumors.<sup>4</sup> When these tumors were irradiated with a single dose of 15 Gy, more tumor-free mice and significant tumor growth delay were observed compared to the split regimen of the same dose ( $3 \times 5$  Gy). After histological analyses of these tumors, the effect on the vasculature was comparable, due to the same application of GET, although the main differences were at the levels of apoptosis and hypoxia.<sup>4</sup> These effects contributed to different IR schedules, where a higher dose was required for the additional activation of the cell death of radioresistant tumors. When the tumors were irradiated with higher doses, for example, 30 Gy, a significant impact on the tumor vasculature was observed. Maeda *et al* showed that such an IR schedule on a dorsal window chamber model resulted in a significant decrease and disruption of smaller tumor blood vessels, while larger tumor blood vessels remained intact. These authors observed reduced tumor viability, although the vasculature began to form organized structures again at 13 days post-IR.<sup>16</sup> These results indicate the restoration of damaged vasculature, which might have also occurred in the present study if the observation time was extended.

Electroporation alone can transiently affect the structure, permeability, and functionality and blood vasculature, and these features are restored within 24 hours.<sup>17</sup> The same finding was also observed in the present study, where the blood vessel area and microcirculation were not significantly affected at 24 hours after the application of pulses. Furthermore, GET promoted vascular targeted effects, which can affect further tumor growth. This result was indicated in a previous study using the same tissue-specific plasmid-silencing endoglin, on tumor growth delay and after histological analysis of tumors, although the precise time scale of the events remained unclear.<sup>4</sup> With intravital microscopy, we observed morphological changes on blood vessels and the significant reduction in the blood vessel area within 24 hours that lasted until the last day of observation, regardless of whether the therapy was combined with IR or not. This effect was strongly correlated with microcirculation measurements, consistent with the findings of other studies, observing tumor vasculature after targeted GET on a dorsal window chamber model, where the reduction in functional vasculature was observed.<sup>6,18</sup>

Combining vascular-modifying agents and IR showed good antitumor effectiveness and can act in an additive or

synergistic manner. In a dorsal window chamber model, the pronounced radiosensibilization was observed after blocking hypoxia inducible factor 1,<sup>19</sup> as well as in a study targeting VEGF receptor 2.<sup>20</sup> Both of these studies used higher IR doses than those used in the present study, and the correlation between tumor vascularization and blood flow obtained by power Doppler sonography was shown in the latter.

Furthermore, the dorsal window chamber model facilitated the daily and noninvasive monitoring of the tumor and its vasculature by simultaneously assessing multiple parameters at the same time. By intravital microscopy, bright-field and fluorescence images were obtained to further calculate and determine the blood vessel area, whereas laser Doppler flowmetry measurements were captured to obtain the blood flow information that indicates blood vessel functionality. The 2 noninvasive methods were used on the same dorsal window chambers, enabling the collection of multiple information from the same animal. The 2 methods additionally confirmed previous observations, indicating a significant vascular-targeted effect of silencing endoglin expression, which occurs within 24 hours after GET. Additionally, the results of these methods highly correlated. Therefore, by measuring the blood vessel area over time, we can indirectly predict the microcirculation dynamics and vice versa. Based on these results, we observed 3 trends: the blood vessel area and microcirculation increased over time in the control groups, whereas in the IR groups, both parameters were stagnating, and in the vascular-targeted groups, the vascularization was completely destroyed.

Both of the methods used in the present study can also be used for the spatial distribution and evaluation of therapies on other nontreated areas. The major common drawback of these 2 methods is the time-consuming process of data acquisition and analysis. Laser Doppler flowmetry was used to confirm the principle and predictions of the correlation of blood vessel area and microcirculation. Techniques, such as laser Doppler imaging and laser speckle contrast imaging, could be used as an alternative to laser Doppler flowmetry, as these methods provide much better spatial and temporal resolution<sup>21,22</sup> and would be better suited for perfusion monitoring but were not available in the present study.

## Conclusion

The GET therapy, where endoglin expression was silenced in a TS/A tumor model, had a vascular-targeted effect. The therapeutic action was detected at 24 hours after therapy and persisted until the end of the observation. The dorsal window chamber model enabled the noninvasive and repeatable acquisition of different information, imaging, and physiological diagnostics at the same time point in the same animal, favoring the 3 R principle of animal welfare. The 2 noninvasive methods used in the present study indicate a good correlation, enabling us to predict the actions of each other by measuring the changes in only one of them.

## Acknowledgments

The authors would like to acknowledge M. Lavric for assistance with cell culture, S. Kos for assistance with animal care, and American Journal Experts (Durham, North Carolina) for the linguistic revision. The authors also acknowledge the financial support from the Slovenian Research Agency (project P3-0003 [Development and evaluation of new approaches to cancer treatment] and research core funding No. J3-6793).


## Declaration of Conflicting Interests


The author(s) declared no potential conflicts of interest with respect to the research, authorship, and/or publication of this article.


## Funding

The author(s) disclosed receipt of the following financial support for the research, authorship, and/or publication of this article: Financial support from the Slovenian Research Agency (project P3-0003 [Development and evaluation of new approaches to cancer treatment] and research core funding No. J3-6793). The study was also conducted in the scope of LEA EBAM (French-Slovenian European Associated Laboratory: Pulsed Electric Fields Applications in Biology and Medicine).

## ORCID iD

Monika Savarin, PhD  <http://orcid.org/0000-0002-8316-8110>

Maja Cemazar, PhD  <http://orcid.org/0000-0002-1418-1928>

Gregor Sersa, PhD  <http://orcid.org/0000-0002-7641-5670>

## References

- Ciric E, Sersa G. Radiotherapy in combination with vascular-targeted therapies. *Radiol Oncol.* 2010;44(2):67-78. doi:10.2478/v10019-010-0025-9.
- El Kaffas A, Tran W, Czarnota GJ. Vascular strategies for enhancing tumour response to radiation therapy. *Technol Cancer Res Treat.* 2012;11(5):421-432. doi:10.7785/tcrt.2012.500265.
- Clémenson C, Chargari C, Deutsch E. Combination of vascular disrupting agents and ionizing radiation. *Crit Rev Oncol Hematol.* 2013;86(2):143-160. doi:10.1016/j.critrevonc.2012.10.002.
- Stimac M, Kamensek U, Cemazar M, Kranjc S, Coer A, Sersa G. Tumor radiosensitization by gene therapy against endoglin. *Cancer Gene Ther.* 2016;23(7):214-220. doi:10.1038/cgt.2016.20.
- Savarin M, Kamensek U, Cemazar M, Heller R, Sersa G. Electrotransfer of plasmid DNA radiosensitizes B16F10 tumors through activation of immune response. *Radiol Oncol.* 2017;51(1):30-39. doi:10.1515/raon-2017-0011.
- Dolinsek T, Markelc B, Sersa G, et al. Multiple delivery of siRNA against endoglin into murine mammary adenocarcinoma prevents angiogenesis and delays tumor growth. *PLoS One.* 2013;8(3):e58723. doi:10.1371/journal.pone.0058723.
- Baron VT, Welsh J, Abedinpour P, Borgström P. Intravital microscopy in the mouse dorsal chamber model for the study of solid tumors. *Am J Cancer Res.* 2011;1(5):674-686.
- Jarm T, Sersa G, Miklavcic D. Oxygenation and blood flow in tumors treated with hydralazine: evaluation with a novel luminescence-based fiber-optic sensor. *Technol Health Care.* 2002;10(5):363-380.
- Jarm T, Podobnik B, Sersa G, Miklavcic D. Effect of hydralazine on blood flow, oxygenation, and interstitial fluid pressure in subcutaneous tumors. *Adv Exp Med Biol.* 2003;510:25-29.
- Kiel JW, Reitsamer HA. *Laser Doppler flowmetry in animals.* In: Schmetterer L, Kiel J, eds. *Ocular Blood Flow.* Berlin, Heidelberg: Springer Berlin Heidelberg; 2012:49-63. doi:10.1007/978-3-540-69469-4\_3.
- Dolinsek T, Markelc B, Bosnjak M, et al. Endoglin silencing has significant antitumor effect on murine mammary adenocarcinoma mediated by vascular targeted effect. *Curr Gene Ther.* 2015; 15(3):228-244. doi:10.2174/1566523215666150126115501.
- Nanni P, de Giovanni C, Lollini PL, Nicoletti G, Prodi G. TS/A: a new metastasizing cell line from a BALB/c spontaneous mammary adenocarcinoma. *Clin Exp Metastasis.* 1983;1(4): 373-380.
- Shepherd AP, Öberg PÅ, eds. *Laser-Doppler Blood Flowmetry.* Vol. 107. Boston, MA: Springer US; 1990. doi:10.1007/978-1-4757-2083-9.
- Folkman J. Angiogenesis: an organizing principle for drug discovery? *Nat Rev Drug Discov.* 2007;6(4):273-286. doi:10.1038/nrd2115.
- Kamensek U, Sersa G, Cemazar M. Evaluation of p21 promoter for interleukin 12 radiation induced transcriptional targeting in a mouse tumor model. *Mol Cancer.* 2013;12(1):136. doi:10.1186/1476-4598-12-136.
- Maeda A, Leung MKK, Conroy L, et al. In vivo optical imaging of tumor and microvascular response to ionizing radiation. *PLoS One.* 2012;7(8):e42133. doi:10.1371/journal.pone.0042133.
- Markelc B, Sersa G, Cemazar M. Differential mechanisms associated with vascular disrupting action of electrochemotherapy: intravital microscopy on the level of single normal and tumor blood vessels. *PLoS One.* 2013;8(3):e59557. doi:10.1371/journal.pone.0059557.
- Bosnjak M, Dolinsek T, Cemazar M, et al. Gene electrotransfer of plasmid AMEP, an integrin-targeted therapy, has antitumor and antiangiogenic action in murine B16 melanoma. *Gene Ther.* 2015; 22(7):578-590. doi:10.1038/gt.2015.26.
- Moeller BJ, Cao Y, Li CY, et al. Inhibition of vascular endothelial growth factor receptor signaling leads to reversal of tumor resistance to radiotherapy. *Cancer Res.* 2004;61(6):2428-2436. doi:10.1016/S0006-3495(93)81326-2.
- Geng L, Donnelly E, McMahon G, et al. Inhibition of vascular endothelial growth factor receptor signaling leads to reversal of tumor resistance to radiotherapy. *Cancer Res.* 2001;61(6): 2413-2419.
- Forrester KR, Stewart C, Tulip J, Leonard C, Bray RC. Comparison of laser speckle and laser Doppler perfusion imaging: measurement in human skin and rabbit articular tissue. *Med Biol Eng Comput.* 2002;40(6):687-697. doi:10.1007/BF02345307.
- Millet C, Roustit M, Blaise S, Cracowski JL. Comparison between laser speckle contrast imaging and laser Doppler imaging to assess skin blood flow in humans. *Microvasc Res.* 2011; 82(2):147-151. doi:10.1016/j.mvr.2011.06.006.